TU Delft

Delft University of Technology

Thermal Stable High-Efficiency Copper Screen Printed Back Contact Solar Cells

Chen, Ning; Rudolph, Dominik; Peter, Christoph; Zeman, Miro; Isabella, Olindo; Rosen, Yitzchak; Grouchko, Michael; Shochet, Ofer; Mihailetchi, Valentin D.

DOI
10.1002/solr.202200874

Publication date
2022

Document Version
Final published version

Published in
Solar RRL

Citation (APA)
Chen, N., Rudolph, D., Peter, C., Zeman, M., Isabella, O., Rosen, Y., Grouchko, M., Shochet, O., & Mihailetchi, V. D. (2022). Thermal Stable High-Efficiency Copper Screen Printed Back Contact Solar Cells. *Solar RRL*, *7 (2023)*(2), 1-9. Article 2200874. https://doi.org/10.1002/solr.202200874

Important note
To cite this publication, please use the final published version (if applicable).
Please check the document version above.

Copyright
Other than for strictly personal use, it is not permitted to download, forward or distribute the text or part of it, without the consent of the author(s) and/or copyright holder(s), unless the work is under an open content license such as Creative Commons.

Takedown policy
Please contact us and provide details if you believe this document breaches copyrights.
We will remove access to the work immediately and investigate your claim.

This work is downloaded from Delft University of Technology.
For technical reasons the number of authors shown on this cover page is limited to a maximum of 10.

Green Open Access added to TU Delft Institutional Repository

'You share, we take care!' - Taverne project

https://www.openaccess.nl/en/you-share-we-take-care

Otherwise as indicated in the copyright section: the publisher is the copyright holder of this work and the author uses the Dutch legislation to make this work public.

Check for updates

Thermal Stable High-Efficiency Copper Screen Printed Back Contact Solar Cells

Ning Chen, Dominik Rudolph, Christoph Peter, Miro Zeman, Olindo Isabella, Yitzchak (Isaac) Rosen, Michael Grouchko, Ofer Shochet, and Valentin D. Mihailetchi**

The high usage of silver in industrial solar cells may limit the growth of the solar industry. One solution is to replace Ag with copper. A screen printable Cu paste is used herein to metallize industrial interdigitated back contact (IBC) solar cells. A novel metallization structure is proposed for making solar cells. Cu paste is applied to replace the majority of the Ag used in IBC cells as busbars and fingers. Cu paste is evaluated for use as fingers, and solar cells are made to test conversion efficiency and reliability. The Cu paste achieves comparably low resistivity, and Cu paste printed cells demonstrate similar efficiency to Ag paste printed cells, with an average efficiency of 23%, and only 4.5 mg W^{-1} of Ag usage. Also, the solar cells are stable and no Cu in-diffusion is observed under damp heat (85 °C, 85% relative humidity) and thermal stress (200 °C) for 1000 h, respectively. All processes used in this study can be carried out with industrial equipment. These findings reveal a new application for Cu pastes and point to a new direction for reducing Ag utilization and cost.

1. Introduction

The photovoltaic (PV) industry has entered the Terawatt (TW) era. As of early 2022, the total PV installation has reached 1 TW.[1] Annual production and installation past TW level is expected in 2030[2] or even earlier in 2028.[3] One of the main concerns for the TW production is the shortage of certain materials.[4] Especially silver (Ag) is one of the key materials used to form electrodes onto silicon solar cells, and mostly applied as paste by screen printing method. For passivated emitter and rear contact (PERC) cells, the Ag consumption is currently around 12 mg W^{-1}.[5] In the case of new emerging industrial solar cells, like heterojunction (HJT) cells and tunnel oxide passivated contact (TOPCon) cells, the Ag consumption is even higher. International Technology Roadmap for Photovoltaic (ITRPV) predicts that the Ag usage for PERC cells will reduce to 7.5 mg W^{-1} within the next 10 years.[5] However, to meet multi-TW production, Zhang et al.[6] proposed that Ag consumption should be reduced to 2 mg W^{-1}. In the near future, if the Ag usage does not decrease, it will not only result in more expensive solar cells, but also limit the sustainable growth of the PV industry.

To reduce the consumption of Ag on solar cells, researchers from industry and institutes are working on different approaches. The first way is to improve the traditional screen design and paste. The use of Ag can be reduced while not compromising cell efficiency, by printing fine lines and improving the finger height-to-width aspect ratio. With advanced screen design, Wenzel et al.[7] reported printed finger width can be reduced to 21 μm with 19 mg Ag paste lay down (without busbar), and the best efficiency group achieved 22.7% efficiency on PERC cells. Second, new equipment is being developed to metallize fine lines. Adrian et al.[8] have reported pattern transfer printing (PTP) with a finger width of 18 μm and an aspect ratio of 0.51. A rotary screen printing method developed by Lorenz et al.[9] has short printing cycles and a low Ag consumption of about 6–9 mg W^{-1}. Schube et al.[10] reported a novel metallization technology called FlexTrail-printing, and very low Ag consumption 0.05 mg W^{-1} has been achieved by using Ag nanoparticle ink. The use of dispensing equipment has also been developed for the metallization of solar cells,[11] with 0.54 mg per Ag finger being reported.[12] The third way is to replace or reduce the use of Ag is to deploy other metals such as copper (Cu). As Cu is an abundant commodity, replacing Ag with Cu will not have an effect on competing technologies.[13] Cu plating is one of the most promising methods of using Cu metallization. In mass production, SunPower/Maxeon has employed Cu plating for many years, resulting in the most efficient and reliable modules in the world.[14] Recent advances have been made on different cell structures[15,16] in labs. Very recently, Sundrive and Maxwell have reported 26.41% record efficiency on large-size heterojunction solar cells by Cu plating.[17]

Despite SunPower/Maxeon's success and excellent lab results, it can be difficult to introduce a new equipment and process into

N. Chen, D. Rudolph, C. Peter, V. D. Mihailetchi
International Solar Energy Research Center (ISC) Konstanz
78467 Konstanz, Germany
E-mail: ning.chen@isc-konstanz.de;
valentin.mihailetchi@isc-konstanz.de

N. Chen, M. Zeman, O. Isabella
Photovoltaic Materials and Devices Group
Delft University of Technology
2628 CD Delft, The Netherlands

Y(Isaac)Rosen, M. Grouchko, O. Shochet
Copprint Technologies Ltd.
Jerusalem 9777518, Israel

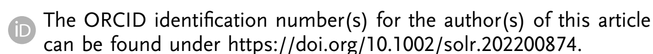

The ORCID identification number(s) for the author(s) of this article can be found under https://doi.org/10.1002/solr.202200874.

DOI: 10.1002/solr.202200874

© 2022 Wiley-VCH GmbH

2367198x, 2023, 2, Downloaded from https://onlinelibrary.wiley.com/doi/10.1002/solr.202200874 by Tu Delft, Wiley Online Library on [02/02/2023]. See the Terms and Conditions (https://onlinelibrary.wiley.com/terms-and-conditions) on Wiley Online Library for rules of use; OA articles are governed by the applicable Creative Commons License

mass production. Manufacturers other than SunPower/Maxeon still have challenges when introducing plating equipment and other new processes. It takes considerable effort and time to evaluate throughput and yield, reduce equipment costs, and reassure environmental concerns regarding the plating process. With the introduction of new equipment with new materials, such as FlexTrail-printing with Ag nanoparticle ink, the challenges will be doubled.

On the other hand, screen printing has proven to be an effective metallization method that is both cost-effective and high-throughput. For industry, it is attractive that Cu can be applied through screen printing. One such application is Ag-coated Cu paste,[18] particularly for HJT cells.[10] By using a coated Ag on Cu particles, the Ag usage can be reduced by 30–50%. A more exciting alternative would be to use a Cu paste that is free of Ag. Previously, Cu paste was successfully used to replace busbar of solar cells.[19,20] Cu pastes were also used as front fingers,[21,22] but either the cell efficiency reported was not as good as reference or was below the state of the art.

In this work, we demonstrate a new method for producing high-efficiency interdigitated back contact (IBC) solar cells using screen printable Cu paste. Our previous study demonstrated that Cu paste can be used as busbar for IBC cells, resulting in high cell efficiency and module reliability.[23] In this study, we replace most of the Ag in IBC cells with Cu paste. An almost fully Cu metallized IBC solar is demonstrated and its efficiency is assessed. The reliability of Cu cells were also evaluated under damp heat conditions (85 °C, 85% relative humidity) and thermal stress at 200 °C for 1000 h, respectively. The findings reveal a new application of Cu pastes to make high-efficiency solar cells and modules, and a new direction for reducing Ag usage.

2. Results and Discussion

2.1. Solar Cell Structure

To use Cu to replace Ag, a properly designed cell structure is needed. The structure of the solar cell used in this study is shown in **Figure 1**a. The solar cells are based on ZEBRA Gen2 cells[24] with a front surface field (FSF). In contrast to standard ZEBRA Gen2 solar cells, the new Cu IBC cells described in this contribution form the local contacts through the dielectric passivation layer stack using a narrow pattern of fire-through Ag paste. The Cu paste fingers are printed in a second printing step in alignment to those Ag contacts. This is achievable by means of a state-of-the-art screen printer. Figure 1b shows a microscope image of a printed Cu finger on Ag contacts. A critical part is the contact area because there Cu diffusion into silicon may occur. To prevent Cu diffusion into silicon, there are two types of measures. First, the locally printed Ag patterns are used for contacting silicon and may also act as barriers between Cu and silicon. Second, the SiO_2/SiN_x stack layers (not visible in the microscopic image) serve both as passivation layers and as barriers. The use of SiN_x has been proven to be an effective barrier to the diffusion of Cu.[25]

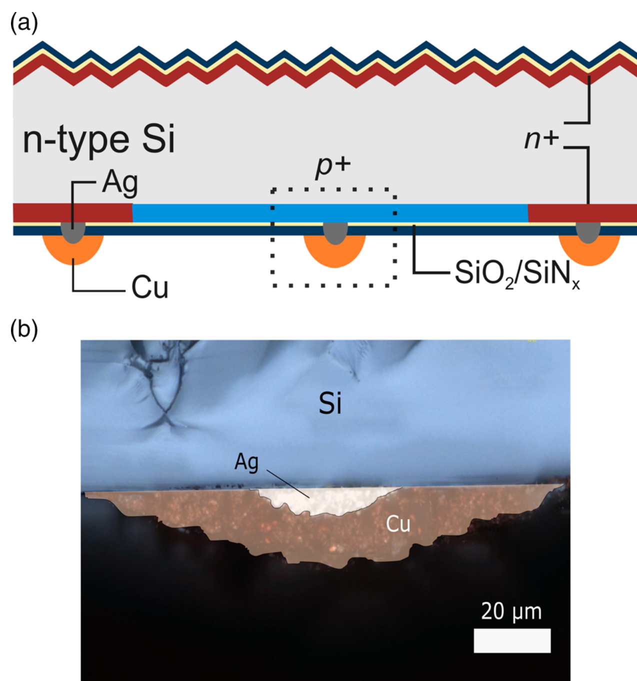

Figure 1. a) Cross-sectional sketch of the ZEBRA IBC solar cell structure used in this study. b) The microscope image of Ag contact coated with Cu finger, corresponding to the dashed area in (a).

2.2. Cu Finger Geometry and Resistance

In this study, Cu pastes were printed as fingers and busbars. In a previous study, we reported results about screen printed Cu busbars on IBC cells.[23] Here, the focus is on Cu paste as fingers. As a reference, a group of IBC cells were screen printed with the baseline Ag paste using the same screen layout. **Figure 2** shows typical microscope images of a finger printed with Cu paste and a finger printed with Ag paste. After printing and curing, the Cu finger has an average width of 125 µm, which is 25 µm wider than the Ag finger. The difference in width is mainly due to the properties of the paste, and the Cu paste spreads more after screen printing. A revised formulation of Cu paste with improved viscosity and thixotropic index for printing fine lines will be tested in the near future. However, the 125 µm finger width is acceptable for use on the rear side of IBC cells in this study. As can be seen by the typical cross-sectional view in Figure 2c, the Cu finger height is approximately 8 µm whereas the Ag finger height is approximately 11 µm. In addition, the Cu finger has a flatter top than the Ag finger, which is related to the different sintering processes used for the two pastes. Overall, the cross-sectional areas of the two pastes are mostly similar.

The line resistance was measured as $0.64 \pm 0.03\ \Omega\,cm^{-1}$ for Cu fingers and $0.35 \pm 0.03\ \Omega\,cm^{-1}$ for Ag fingers. As the cross-sectional areas of the two pastes are similar, the differences in line resistance are primarily due to differences in the resistivity of the pastes. Based on the line resistance and the cross-sectional area, we have calculated that the Cu resistivity is approximately $5 \times 10^{-6}\ \Omega\,cm$. This result is superior to the previous reported values for a Cu paste,[26,27] which were

© 2022 Wiley-VCH GmbH

2367198x, 2023, 2, Downloaded from https://onlinelibrary.wiley.com/doi/10.1002/solr.202200874 by Tu Delft, Wiley Online Library on [02/02/2023]. See the Terms and Conditions (https://onlinelibrary.wiley.com/terms-and-conditions) on Wiley Online Library for rules of use; OA articles are governed by the applicable Creative Commons License

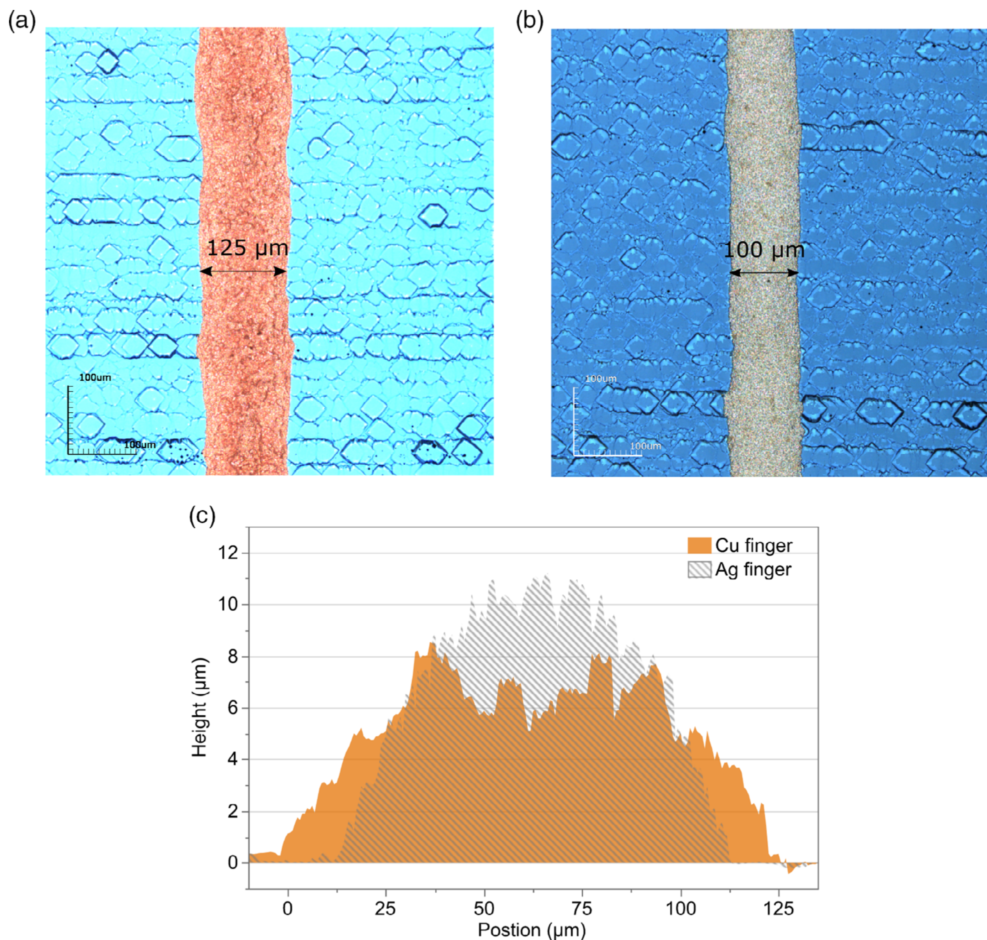

Figure 2. A microscope snapshot of a typical a) printed Cu finger and b) printed Ag finger on the IBC cells. c) Typical cross sections of a Cu finger and a Ag finger.

annealed at a higher temperature in nitrogen or in vacuum. The solar cell results are shown in the next subsection.

2.3. Solar Cell Results

A batch of IBC solar cells precursors were identically fabricated up to the metallization step. A first layer of Ag fire-through paste was then screen printed using a point contact pattern and fired in a fast firing furnace according to our best known method. Subsequently the cells were randomly distributed in two groups as follow: a Ag group of cells that were printed with Ag fingers and Ag busbars, and a Cu group of cells that were printed with Cu fingers and Cu busbars.

Figure 3 illustrates the parameters extracted from current–voltage (I–V) characteristics of all cells under the standard test conditions (STC). I–V results are also summarized in **Table 1** along with their averages and standard deviations. In both groups, V_{oc} values are similar, with an average V_{oc} of around 689 mV. Compared to the Ag group, the Cu group has a lower average J_{sc} of 0.1 mA cm^{-2}. Cells with median J_{sc} were measured for quantum efficiency (QE), and the results are shown in **Figure A1**. In long wavelength range, QE and reflectance curves are similar for Ag cell and Cu cell. There were slightly higher QE curves measured on Ag cells in the wavelength range between 400 and 1000 nm. The results suggest that the difference in J_{sc} may be caused by factors other than pastes (e.g., difference in wafer bulk lifetime). In terms of fill factor (FF), the Cu cells exhibit a 0.3%$_{abs}$ higher FF on average than that of the Ag cells. However, compared to the standard deviations, the differences between the groups were not statistically significant. It is worth noting that the Ag cells were fired twice (contact and fingers, respectively), and the two firing steps need to be carefully tuned to get an optimal FF. In contrast, Cu cells require only one firing step, which makes it easier to optimize the firing process and improve the FF in the future. At last, in terms of cell efficiency, same efficiency was achieved for both the Cu metallized group and the reference Ag metallized group. The average efficiency of Cu cells group (34 cells) was 23%, with the best cell efficiency of 23.25%.

By using Cu paste, the Ag consumption was reduced to 25 mg for a 6 inch M2 wafer (our best result so far), which is less than 4.5 mg W^{-1}. Compared to current state-of-the-art PERC cells, which use approximately 12 mg W^{-1} Ag, the Ag consumption was reduced by over 60%. Moreover, Ag

 © 2022 Wiley-VCH GmbH

2367198x, 2023, 2, Downloaded from https://onlinelibrary.wiley.com/doi/10.1002/solr.202200874 by Tu Delft, Wiley Online Library on [02/02/2023]. See the Terms and Conditions (https://onlinelibrary.wiley.com/terms-and-conditions) on Wiley Online Library for rules of use; OA articles are governed by the applicable Creative Commons License

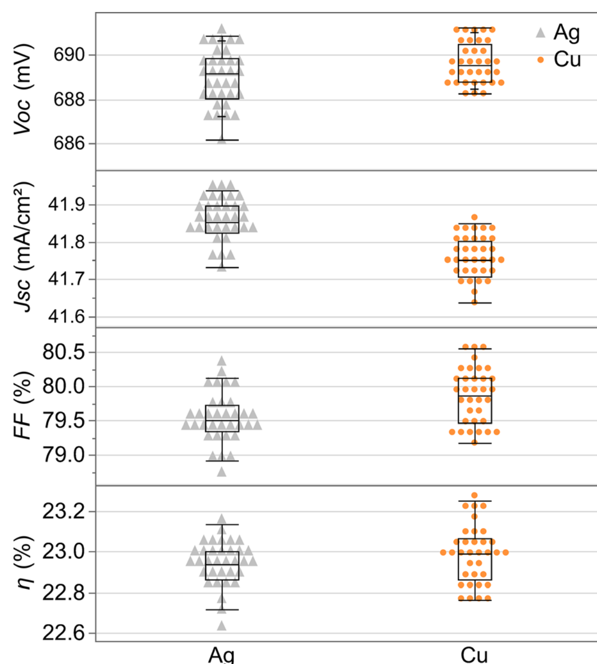

Figure 3. *I–V* results of solar cells made using Ag and Cu pastes. In the box-and-whisker plots, the box shows the median, 25 and 75th percentiles, and the whiskers are minimum and maximum data values excluding outliers.

Table 1. *I–V* summary of Cu and Ag printed cells.

Paste	Data type	V_{oc} [mV]	J_{sc} [mA cm^{-2}]	FF [%]	η [%]
Ag	Best cell	687.2	41.92	80.32	23.14
	Avg. of 34 cells	688.9 ± 1.2	41.85 ± 0.05	79.54 ± 0.36	22.94 ± 0.11
Cu	Best cell	690.2	41.80	80.56	23.25
	Avg. of 34 cells	689.6 ± 0.9	41.75 ± 0.06	79.81 ± 0.41	22.98 ± 0.13

consumption can be further reduced by printing thinner and smaller layers of Ag.

2.4. Reliability of Damp Heat Test

Besides the efficiency of the solar cell, the main concern for Cu metallized cells and modules is their reliability. In spite of this, there are no standards specifically designed for testing Cu paste printed solar cells. In accordance with IEC standard 61 215, damp heat (DH) and thermal cycling (TC) tests are the most relevant tests. As described in our previous study,[23] we demonstrated that after DH3000 and TC600 the modules with Cu busbars show no sign of cells degradation due to Cu in-diffusion. Several minimodules with Cu metallization of both fingers and busbars were also tested for DH in this study. We skipped TC tests because they were more related to interconnections, which have already been tested for Cu busbar.[23] For DH test, the minimodules were manufactured with different combinations, including glass-backsheet (BS) structures with ethylene vinyl acetate (EVA) encapsulation, and glass–glass structures with polyolefin elastomer (POE) encapsulation, as detailed in the Experimental Section. As we are still working on improving the peel force of soldering method, we used electrically conductive adhesives (ECA) to make minimodules in this experiment. The Ag-containing ECA was used to demonstrate the reliability of Cu cells in the experiment. In mass production, either ECA can be used (in this case, the Ag usage in ECA should also be considered[6]), or Ag-free solutions such as soldering with SnPb ribbon can be employed (in development).

Figure 4 illustrates the normalized *I–V* parameters and pFF changes of different minimodules during the 1000 h DH test. Three types of minimodules were tested, including Cu cells encapsulated in POE and glass–glass (POE/glass), in EVA and glass-backsheet (EVA/BS), and reference Ag cells encapsulated in EVA and glass-backsheet (EVA/BS). One of the unexpected findings is the increase in FF observed in the Cu groups. FF of Cu modules with EVA/BS increased until around DH200 and then decreased whereas the FF of Cu modules with POE/Glass increased by approx. 10% and remained stable. On the other hand, the FF of reference Ag modules remained unchanged during the test. An unexpected observation is that the initial FF of Cu modules was low around 70%, while Ag modules had a high FF of around 78%. Electroluminescence (EL) images indicate that the low initial FF of Cu modules is due to poor interconnection between Cu paste and ECA Photoluminescence (PL) and EL results are shown in **Figure 5**. During the DH test, the FF of Cu cells increased or decreased due to changes in the interconnection between Cu busbar and ECA It is not yet clear what the underlying cause is. For all groups, the V_{oc} and pFF remain stable during the test. For the Cu groups, there was even a small increase in pFF. The pFF increased by 0.4 and 0.2%$_{rel}$ for the EVA/BS and POE/Glass groups, respectively. From these stable pFF and V_{oc} results, we can conclude that there is no Cu in-diffusion observed during the DH1000 test.

2.5. Stability under Thermal Stress

For commercial modules, manufacturers generally provide a warranty of 25 years or longer. That means modules should retain at least 80% of their original power generation capacity after 25 years. However, it should be noted that the "standard module qualification test results cannot be used to obtain or infer a product lifetime."[28] To test the long-term reliability of Cu metallized cells, additional accelerated tests are required. According to Bartsch et al., stability under thermal stress can be estimated by fitting pFF loss measurement data at different temperatures using the Arrhenius plot.[29] Our study, however, did not observe obvious pFF losses from the high-temperature degradation test at 200 °C, so it was not possible to use this method.

Alternatively, the long-term stability of the cells can be determined by using the Arrhenius model, using the equation[30]

$$\frac{t(T_{use})}{t(T_{acc})} = \exp\left[\frac{E_a}{k}\left(\frac{1}{T_{use}} - \frac{1}{T_{acc}}\right)\right] \quad (1)$$

In the equation, T_{use} is the device's operating temperature, T_{acc} is the acceleration testing temperature, k is the Boltzmann constant, and E_a is the activation energy; the device working time

© 2022 Wiley-VCH GmbH

2367198x, 2023, 2, Downloaded from https://onlinelibrary.wiley.com/doi/10.1002/solr.202200874 by Tu Delft, Wiley Online Library on [02/02/2023]. See the Terms and Conditions (https://onlinelibrary.wiley.com/terms-and-conditions) on Wiley Online Library for rules of use; OA articles are governed by the applicable Creative Commons License

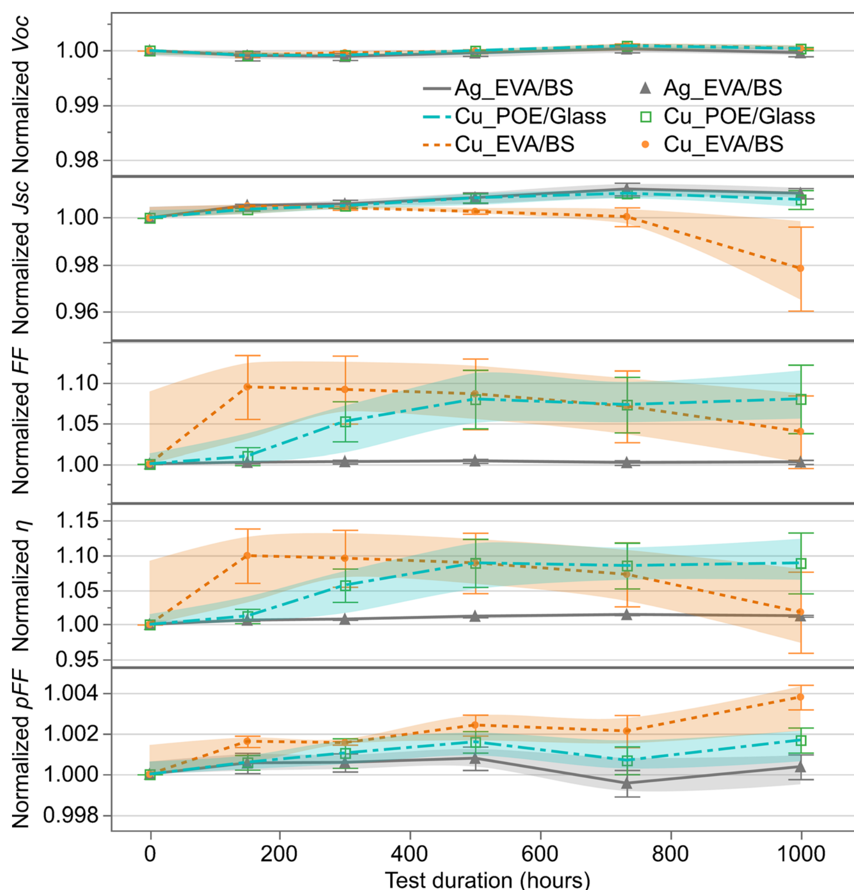

Figure 4. Normalized *I–V* parameters and pFF changes of different minimodules during 1000 h DH exposure. Three types of minimodules were tested, including Cu cells encapsulated in POE and glass–glass (POE/glass), in EVA and glass-backsheet (EVA/BS), and reference Ag cells encapsulated in EVA and glass-backsheet (EVA/BS). The values are averages of 3 samples with the error bar representing one standard deviation, and the shaded areas indicate the 95% confidence interval.

(e.g., 25 years) is represented as $t(T_{use})$, and the corresponding testing time is $t(T_{acc})$.

One of the challenges of using this method is the difficulty in determining the activation energy. Similar to a previous study,[31] we used here the activation energy as suggested in the standard of the European Cooperation for Space Standardization (ECSS) for photovoltaic assemblies and components (ECSS-E-ST-20-08C Rev.1).[32] The standard assumes an activation energy of 0.70 eV, which applies to "crystalline silicon and single and multijunction GaAs solar cells with a thickness of more than 50 μm."

By using Equation (1) and activation energy of $E_a = 0.70$ eV, the temperature and time required to conduct an accelerate test can be calculated. **Figure 6** shows the estimated temperature and time needed for acceleration test based on different working temperatures for 25 years. For example, the green curve at lowest position assumes that the modules working temperature is 45 °C (typical working temperature stated in the module datasheet, also called nominal module operation temperature [NMOT]) for 25 years, and that the acceleration test should take place for 50 h at 200 °C. For worse-case scenarios, the working temperatures of 55, 65, 75, and 85 °C are also provided. As a worst case scenario, for example, 85 °C for 25 years, the acceleration test should be carried out for 900 h at 200 °C. With a higher test temperature, such as 250 °C, the acceleration testing time can be significantly reduced.

In this study, we considered a worst case scenario by testing the Cu cells at 200 °C for 1000 h, which is equivalent to a module working at 85 °C for more than 25 years. The temperature of 200 °C was chosen because the cell structure of the IBC cells will not be damaged at this temperature. Also, 1000 h is an acceptable time frame for testing, which can be completed within 2 months, including characterization. Four groups of samples were measured: two groups underwent the 200 °C thermal stress testing, and two reference groups were kept at room temperature. The test results are shown in **Figure 7**, which includes the two most degradation sensitive cell parameters—V_{oc} and pFF. During these tests, the reference groups with Ag or Cu paste showed stable V_{oc}; the fluctuations were only due to measurement errors. A slight reduction in V_{oc} was observed for test groups of Ag and Cu cells. For Cu cells, a degradation in V_{oc} of only around 0.5%$_{rel}$ or 3.4 mV was observed. Additionally, the PL results shown in **Figure A2** confirm the V_{oc} results on Cu and Ag tested cells. In terms of pFF changes, the reference groups are stable with no change after 1000 h. After 1000 h of accelerating temperature

© 2022 Wiley-VCH GmbH

2367198x, 2023, 2, Downloaded from https://onlinelibrary.wiley.com/doi/10.1002/solr.202200874 by Tu Delft, Wiley Online Library on [02/02/2023]. See the Terms and Conditions (https://onlinelibrary.wiley.com/terms-and-conditions) on Wiley Online Library for rules of use; OA articles are governed by the applicable Creative Commons License

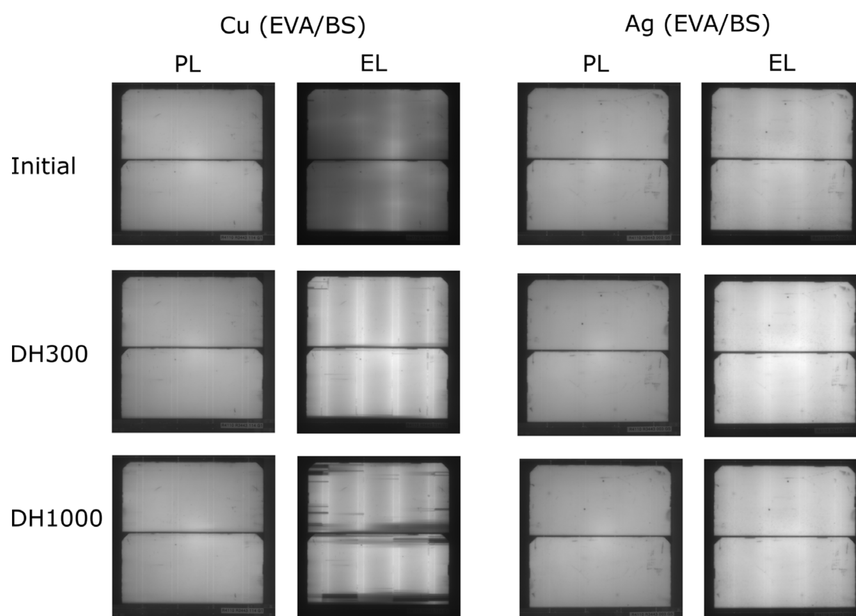

Figure 5. PL and EL images of Cu metallized (left columns) and Ag metallized (right columns) samples measured at the initial stage, 300, and 1000 h after damp heat test.

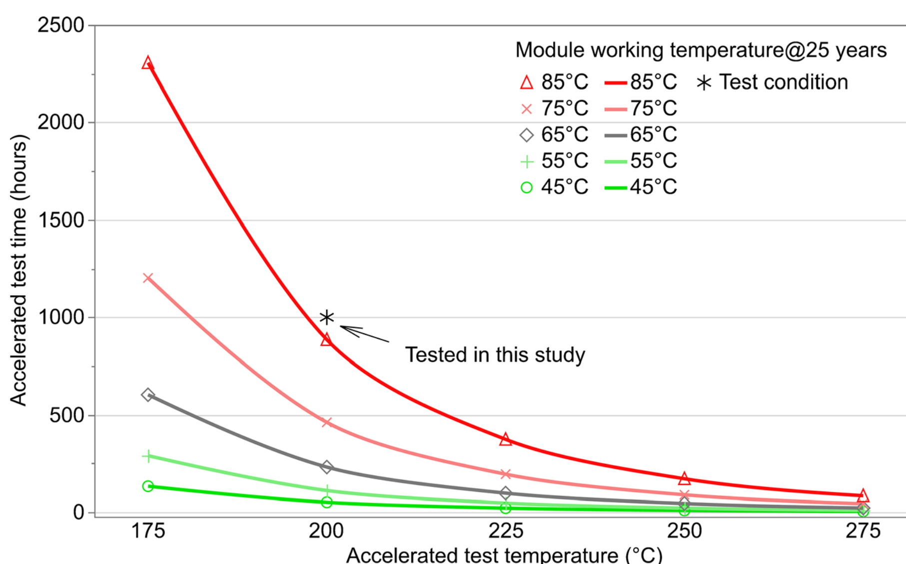

Figure 6. Calculated accelerated thermal stress test temperature (*x*-axis) and time (*y*-axis) according to the different module operating temperatures (shown in the legend). Conditions with 1000 h at 200 °C were tested in this study, shown as asterisk.

test, the decrease in pFF for the Cu printed group is less than $0.5\%_{rel}$, indicating that there is no sign of Cu diffusion into the silicon during this time period, which would otherwise resulted in significantly higher pFF degradation.[25] Moreover, this is demonstrated also by the reference Ag group results, which show similar or slightly higher pFF loss during the test.

In summary, there was no measurable pFF degradation observed in these accelerated stress tests, which indicates that no Cu diffusion took place into the silicon. The pFF losses of Cu cells are comparable to previous reports with thick nickel barriers on plated Cu cells.[25] The screen printed fire-through Ag paste served as an effective barrier. Cu diffusion may be inhibited by the paste constituents (particularly the glass frit). Similarly, in a report from Kraft et al.,[33] Ag pastes were used as seed layers for Cu-plated cells, and the seed layer was also noticed as a barrier which may be related to the paste composition. In our study, the additives present in the Cu paste prevented oxidation. During the solar cell process, the Cu paste remained stable. No oxidation occurred during the curing process even when the process temperature was elevated to 300 °C (as determined by the paste resistivity and color). In a recent report, a Cu paste was even used to directly contact the front side of p-PERC

 © 2022 Wiley-VCH GmbH

2367198x, 2023, 2, Downloaded from https://onlinelibrary.wiley.com/doi/10.1002/solr.202200874 by Tu Delft, Wiley Online Library on [02/02/2023]. See the Terms and Conditions (https://onlinelibrary.wiley.com/terms-and-conditions) on Wiley Online Library for rules of use; OA articles are governed by the applicable Creative Commons License

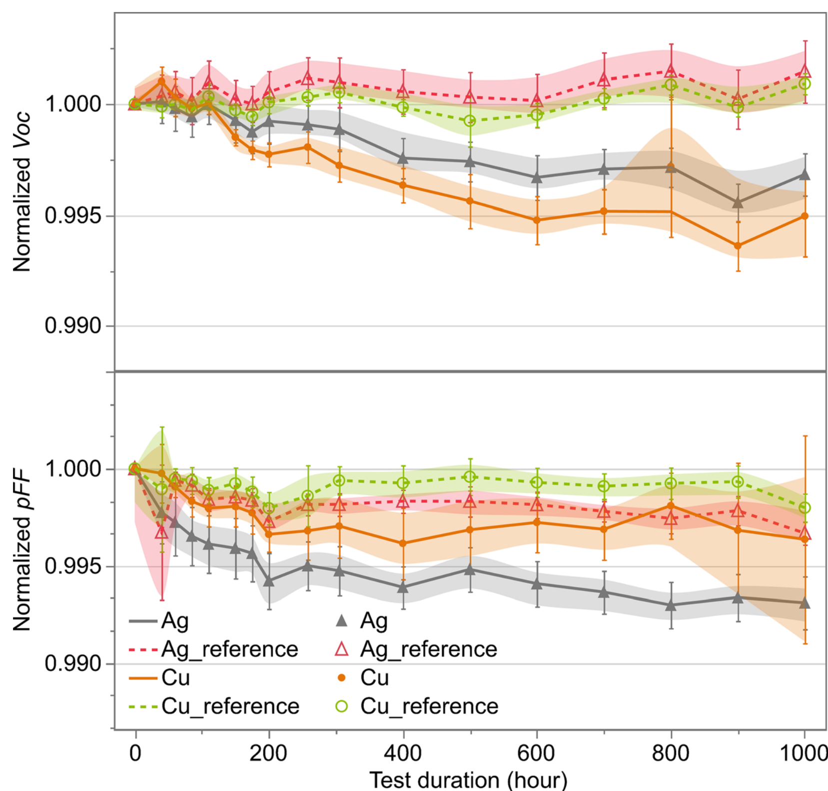

Figure 7. Results of normalized V_{oc} and pFF of different groups, including Ag cells (Ag) and Cu cells (Cu) exposed to 1000 h of 200 200 °C, as well as reference groups with Ag cells (Ag_reference) and Cu cells (Cu_reference) kept at room temperature. The values are averages of 3 to 5 samples with the error bar representing 1 standard deviation, and the shaded areas indicate the 95% confidence interval.

cells with no barriers.[34] Screen printed Cu pastes for metallization of solar cells are attracting researchers' attention. In contrast to the extensively studied plated Cu,[35] more research is needed on screen printed Cu pastes and cells, notably on the contact formation and diffusion of Cu and their impact on long-term stability.

3. Conclusion

In this study, a screen printed Cu paste was used as a conductive layer for IBC cells in order to replace the majority of Ag utilization. The cells were printed using two layers—a thin fire-through Ag paste was printed first, followed by Cu paste applied as fingers and busbars. The Cu paste printed cells achieve the same level of efficiency as the reference fully Ag paste printed cells, both groups achieving average efficiencies of 23%. Cu paste replaced most of the Ag usage in the cells, resulting in a Ag consumption of only 4.5 mg W^{-1}. In addition, reliability and stability were examined. There was no degradation in V_{oc} and pFF during the damp heat stress test (85 °C, 85% relative humidity) of 1000 h. Under more severe test conditions—a thermal stress test under 200 °C for 1000 h—V_{oc} of Cu cells only degraded by 0.5%$_{rel}$ and pFF only by 0.3%$_{abs}$. The reliability and stability results convincingly show that Cu diffusion into Si bulk from a screen printed paste can be prevented. The findings of this study demonstrate that the screen printed Cu paste has an immediate potential to replace most of the Ag used for metallization of an industrial cell concept.

4. Experimental Section

Solar Cell Fabrication: The solar cells were fabricated based on ZEBRA Gen2 cells process flow,[24] on 175 μm thick, n-type 6 inch wafers with a base resistivity of 6 ± 3 Ω cm. The front/back surface field (FSF/BSF) and rear emitter regions are formed in industrial tube diffusion furnaces using $POCl_3$ and BBr_3 as the diffusion sources, respectively. A plasma-enhanced chemical vapor deposition (PECVD) mask layer of SiN_x and a 532 nm nanosecond laser were used to form the interdigitated patterns on the rear side. The passivation and antireflection coating (ARC) layers were formed by a stacked layer structure comprising thermal SiO_2-grown in situ during the diffusion process and capped with SiN_x.[36] Finally, metallization was accomplished by screen printing 3D metallization patterns comprising busbars, fingers, and isolation layers. The solar cells were fabricated in the mass production line until the metallization step. For metallization, two groups of cells were made—Cu and Ag cells. Both cells were printed with point contact Ag pattern of a fire-through Ag paste, and dried at around 200 °C followed by high-temperature firing process at around 800 °C to form the local Ag–Si contacts. In a second printing step, for Cu group, wider Cu paste fingers are printed in alignment to the Ag point contacts whereas for Ag groups the Ag fingers are printed. The Cu paste was dried at 100 °C for 30 s and then annealed at 300 °C for 5 s in a lamination machine. The Ag group was printed with a nonfire-through Ag paste, dried, and fired in an inline furnace at around 700 °C for a few seconds. Then an insulation paste was printed for both groups and dried. After applying the insulation paste pattern, the busbars pairs are printed

© 2022 Wiley-VCH GmbH

2367198x, 2023, 2, Downloaded from https://onlinelibrary.wiley.com/doi/10.1002/solr.202200874 by Tu Delft, Wiley Online Library on [02/02/2023]. See the Terms and Conditions (https://onlinelibrary.wiley.com/terms-and-conditions) on Wiley Online Library for rules of use; OA articles are governed by the applicable Creative Commons License

by either Cu paste or Ag paste to interconnect the p-type and n-type fingers, completing the multilayer metallization pattern. The Cu paste used in the experiment, LF-371, was provided by Copprint Technologies Ltd. and all pastes used in this study are commercially available.

Minimodules Fabrication and Reliability Tests: Minimodules were made from two pieces of half-cut cells for damp heat testing. Before module processing, the solar cells were cut into half cells by a 1064 nm laser (Rofin F20). For making modules, the ECA (Henkel) was dispensed on the busbar of cells (Stepcraft). Ribbons were placed on ECA and fixed to the cells, and then curing at 140 °C for 7 min on a hot plate. String connectors were connected to the ribbons by soldering.[37] Encapsulation films (EVA or POE), front glasses, and backsheets or rear glasses were used to encapsulate the cells, and then laminated in a laminator (Phototrade—P. Energy) with recipes for EVA/backsheet, or POE/double-glass modules.

The minimodules were tested under damp heat conditions for 1000 h in a climate chamber (Vötsch) according to the IEC-61215 standard.[38] For the high-temperature thermal stress test, half cut cells were used. The cells were placed between two pieces of glass, and put into a muffle furnace (Nabertherm). Then the cells were heated and annealed at a set temperature of 200 °C under N_2 flow in order to minimize oxidation. The modules or cells were taken out the climate chamber or furnace and cooled down to room temperature for measurement at different time intervals.

Characterization: One sun *I–V* characterization was performed using a Class AAA xenon flasher (halm elektronik). Before measurement, the I_{sc} was calibrated by using a calibration cell or module (Fraunhofer ISE CalLab). The finger height, width, and cross-sectional area were analyzed using a laser scanning microscope (LSM, Olympus). The finger line resistance is calculated from busbar to busbar resistance which is measured from a resistance tester (ECN). PL and EL were measured using in-house developed equipment (ISC Konstanz). pFF and V_{oc} were from Suns-V_{oc} measurement,[39] using an in-house developed chuck for IBC cells.

Appendix A

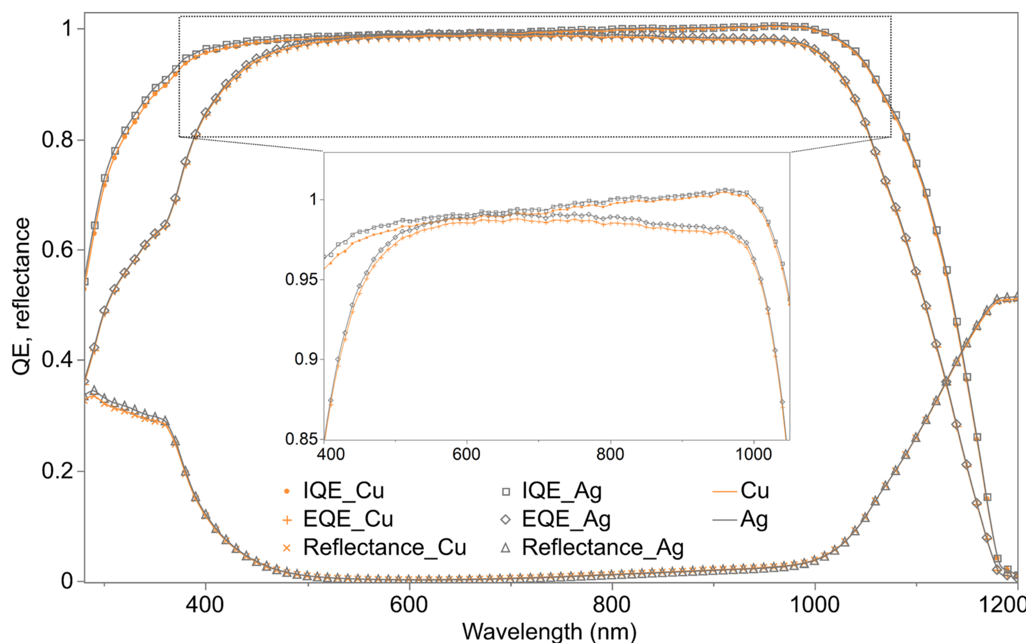

Figure A1. QE and reflectance curves of Cu and Ag solar cells with median I_{sc} selected from each group. From 400 nm to 1000 nm, the Ag cell exhibits better QE.

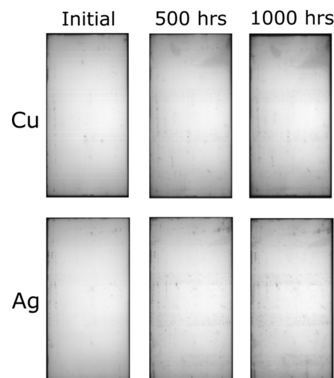

Figure A2. PL images of Cu cell (top) and Ag cell (bottom) at the initial stage of heat stress, exposed to 200 °C for 500 and 1000 h, respectively.

Acknowledgements

This work was supported by the German Federal Ministry for Economic Affairs and Climate Action (BMWK) as part of the FlexFab 2 project with funding reference numbers 03EE1081B.

Conflict of Interest

The authors declare no conflict of interest.

Data Availability Statement

The data that support the findings of this study are available from the corresponding author upon reasonable request.

© 2022 Wiley-VCH GmbH

2367198x, 2023, 2, Downloaded from https://onlinelibrary.wiley.com/doi/10.1002/solr.202200874 by Tu Delft, Wiley Online Library on [02/02/2023]. See the Terms and Conditions (https://onlinelibrary.wiley.com/terms-and-conditions) on Wiley Online Library for rules of use; OA articles are governed by the applicable Creative Commons License

Keywords

back contacts, copper paste, screen printing, silver reduction, solar cells, thermal stability

Received: September 27, 2022
Revised: November 14, 2022
Published online: November 30, 2022

[1] pv. magazine, World has Installed 1 TW of Solar Capacity, https://www.pv-magazine.com/2022/03/15/humans-have-installed-1-terawatt-of-solar-capacity/ (accessed: September 2022).
[2] pv. magazine, Global Annual Solar Deployment to Hit 1 TW by 2030, https://www.pv-magazine.com/2022/05/17/global-annual-solar-deployment-to-hit-1-tw-by-2030/ (accessed: September 2022).
[3] J. Kopecek, R. Libal, *Photovoltaics Int.* **2022**, *48*, 60.
[4] P. J. Verlinden, *J. Renewable Sustainable Energy* **2020**, *12*, 5.
[5] J. Trube, *International Technology Roadmap for Photovoltaic (itrpv): 2021 Results, Report, VDMA Photovolt. Equipment*, https://www.vdma.org/international-technology-roadmap-photovoltaic (accessed: September 2022).
[6] Y. Zhang, M. Kim, L. Wang, P. Verlinden, B. Hallam, *Energy Environ. Sci.* **2021**, *14*, 5587.
[7] T. Wenzel, A. Lorenz, E. Lohmüller, S. Auerbach, K. Masuri, Y. C. Lau, S. Tepner, F. Clement, *Sol. Energy Mater. Sol. Cells* **2022**, *244*, 111804.
[8] A. Adrian, D. Rudolph, N. Willenbacher, J. Lossen, *IEEE J. Photovoltaics* **2020**, *10*, 1290.
[9] A. Lorenz, M. Klawitter, M. Linse, L. Ney, S. Tepner, S. Pingel, M. S. Sabet, J. Reiner, K. Oehrle, R. Greutmann, J. Röth, M. Drews, K. Muramatsu, S.-I. Ikarashi, F. Clement, *Energy Technol.* **2022**, *10*, 8.
[10] J. Schube, T. Fellmeth, M. Jahn, R. Keding, S. W. Glunz, *Phys. Status Solidi RRL* **2019**, *13*, 9.
[11] M. Pospischil, T. Riebe, A. Jimenez, M. Kuchler, S. Tepner, T. Geipel, D. Ourinson, T. Fellmeth, M. Breitenbücher, T. Buck, M. Dhamrin, F. Clement, *AIP Conf. Pro.* **2019**, *2156*, 020005.
[12] K. Gensowski, M. Much, E. Bujnoch, S. Spahn, S. Tepner, F. Clement, *Sci. Rep.* **2022**, *12*, 12318;
[13] M. A. P. Macé, E. Bosch, in *38th European Photovoltaic Solar Energy Conf. and Exhibition*, ISBN 3-936338-78-7 **2021**, pp. 683–689.
[14] SunPower Whitepaper, Sunpower Module 40-Year Useful Life, Report, https://us.sunpower.com/sites/default/files/media-library/white-papers/wp-sunpower-module-40-year-useful-life.pdf (accessed: September 2022).
[15] C. Han, G. Yang, P. Procel, D. O'Connor, Y. Zhao, A. Gopalakrishnan, X. Zhang, M. Zeman, L. Mazzarella, O. Isabella, *Sol. RRL* **2022**, *6*, 6.
[16] B. Grübel, G. Cimiotti, C. Schmiga, S. Schellinger, B. Steinhauser, A. A. Brand, M. Kamp, M. Sieber, D. Brunner, S. Fox, S. Kluska, *Prog. Photovoltaics Res. Appl.* **2021**, *30*, 615.
[17] pv. magazine, Sundrive Achieves 26.41% Efficiency with Copper-Based Solar Cell Tech, https://www.pv-magazine.com/2022/09/05/sundrive-achieves-26-41-efficiency-with-copper-based-solar-cell-tech/ (accessed: September 2022).
[18] J. Shin, H. Kim, K. H. Song, J. Choe, *Chem. Lett.* **2015**, *44*, 1223.
[19] S. Yoshiba, M. Dhamrin, M. Yoshida, A. Uzum, U. Itoh, H. Tokuhisa, S. Sekine, T. Saitoh, K. Kamisako, in *27th European Photovoltaic Solar Energy Conf. and Exhibition*, Frankfurt, Germany **2012**, pp. 1730–1732.
[20] D. Wood, I. Kuzma-Filipek, R. Russell, F. Duerinckx, N. Powell, A. Zambova, B. Chislea, P. Chevalier, C. Boulord, A. Beucher, N. Zeghers, W. Deng, Z. Feng, P. Verlinden, J. Szlufcik, G. Beaucarne, *Energy Procedia* **2014**, *55*, 724.
[21] T. Druffel, R. Dharmadasa, K. Ankireddy, K. Elmer, A. Ebong, S. Huneycutt, in *47th IEEE Photovoltaic Specialists Conf. (PVSC)*, IEEE, Piscataway, NJ **2020**.
[22] K. Gawlinska-Necek, R. P. Socha, P. Balawender, M. K. Stodolny, B. B. Van Aken, Z. Starowicz, P. Panek, *Prog. Photovoltaics Res. Appl.* **2021**, *29*, 1008.
[23] D. Rudolph, R. Farneda, T. Timofte, A. Halm, N. Chen, J. Libal, F. Buchholz, I. Rosen, M. Grouchko, O. Shochet, in *AIP Conf. Pro.* **2022**, *2709*, 020006.
[24] R. Kopecek, J. Libal, J. Lossen, V. D. Mihailetchi, H. Chu, C. Peter, F. Buchholz, E. Wefringhaus, A. Halm, J. Ma, L. Jianda, G. Yonggang, Q. Xiaoyong, W. Xiang, D. Peng, in *47th IEEE Photovoltaic Specialists Conf. (PVSC)*, Online, IEEE, Piscataway, NJ **2020**, pp. 1008–1012.
[25] A. Kraft, C. Wolf, J. Bartsch, M. Glatthaar, S. Glunz, *Sol. Energy Mater. Sol. Cells* **2015**, *136*, 25.
[26] J. Tang, C. H. H. Mak, S. K. Tam, K. M. Ng, *J. Nanopart. Res.* **2021**, *23*, 8.
[27] B. H. Teo, A. Khanna, V. Shanmugam, M. L. O. Aguilar, M. E. Delos Santos, D. J. W. Chua, W.-C. Chang, T. Mueller, *So. Energy* **2019**, *189*, 179.
[28] C. R. Osterwald, T. J. McMahon, *Prog. Photovoltaics Res. Appl.* **2009**, *17*, 11.
[29] J. Bartsch, A. Mondon, K. Bayer, C. Schetter, M. Hörteis, S. W. Glunz, *J. Electrochem. Soc.* **2010**, *157*, 10.
[30] N. Núñez, J. R. González, M. Vázquez, C. Algora, P. Espinet, *Prog. Photovoltaics Res. Appl.* **2013**, *21*, 5.
[31] R. van Leest, G. Bauhuis, P. Mulder, R. van der Heijden, E. Bongers, E. Vlieg, J. Schermer, *Sol. Energy Mater. Sol. Cells* **2015**, *140*, 45.
[32] ECSS, Ecss-e-st-20-08c rev.1 – photovoltaic Assemblies and Components **2012**.
[33] A. Kraft, C. Wolf, J. Bartsch, M. Glatthaar, *Energy Procedia* **2015**, *67*, 93.
[34] A. Ebong, S. Huneycutt, S. Grempels, K. Ankireddy, R. Dharmadasa, T. Druffel, in *2021 IEEE 48th Photovoltaic Specialists Conf. (PVSC)*, IEEE, Piscataway, NJ **2021**, pp. 1417–1420.
[35] G. Cimiotti, J. Bartsch, A. Kraft, A. Mondon, M. Glatthaar, *Energy Procedia* **2015**, *67*, 84.
[36] V. D. Mihailetchi, H. Chu, J. Lossen, R. Kopecek, *IEEE J. Photovoltaics* **2018**, *8*, 435.
[37] T. Meßmer, F. Demiralp, A. Halm, *Energy Procedia* **2016**, *98*, 98.
[38] IEC, *Crystalline Silicon Terrestrial Photovoltaic (PV) Modules: Design Qualification and Type Approval* **2021**.
[39] A. C. Ronald, A. Sinton, in *16th European Photovoltaic Sol. Energy Conf.*, Glasgow, UK **2000**, pp. 1152–1155.

 © 2022 Wiley-VCH GmbH

2367198x, 2023, 2, Downloaded from https://onlinelibrary.wiley.com/doi/10.1002/solr.202200874 by Tu Delft, Wiley Online Library on [02/02/2023]. See the Terms and Conditions (https://onlinelibrary.wiley.com/terms-and-conditions) on Wiley Online Library for rules of use; OA articles are governed by the applicable Creative Commons License